Title Page

Variations of photosynthetic N-use efficiency through plant phylogeny in relation to mesophyll cell wall thickness

Dan-dan Liu[1†], Xiao Song[1], Tiina Tosens[2], Dong-liang Xiong[3], Marc Carriquí[4], You-cai Xiong[1], Wei Xue[1*,†]

[1]College of Ecology, State Key Laboratory of Grassland Agroecosystems, Lanzhou University, Lanzhou 730000, China

[2]Institute of Agricultural and Environmental Sciences, Estonian University of Life Sciences, Kreutzwaldi, Tartu 51014, Estonia

[3]National Key Laboratory of Crop Genetic Improvement, Hubei Hongshan Laboratory, MOA Key Laboratory of Crop Ecophysiology and Farming System in theMiddle Reaches of the Yangtze River, Huazhong Agricultural University, Wuhan 430070, China

[4]Research Group on Plant Biology under Mediterranean Conditions, Institut d'Investigacions Agroambientals i d'Economia de l'Aigua (INAGEA) – Universitat de les Illes Balears (UIB), Ctra Valldemossa Km 7.5., 07122, Illes Balears, Spain

*Corresponding author: W. Xue (xuewei@lzu.edu.cn), Tel: 0931-8915950

†These authors contributed equally to this work

Running head: cell wall thickness constrains PNUE along plant's phylogeny

Abstract Photosynthetic nitrogen-use efficiency (PNUE) varied greatly among C_3 species. Previous studies suggested that PNUE patterns in spermatophyta are characterized in relation to leaf mass per area (LMA) and explained by the LMA-mediated tradeoffs between N allocation to cell walls and Rubisco and mesophyll conductance (g_m). However, morpho-physiological mechanisms and interrelationships shaping PNUE remain unclear at an evolutionary time scale. Here, we compiled a novel large matrix of leaf morpho-anatomical and physiological traits in 679 C_3 species from bryophytes to angiosperm to further understand the complexity of interrelationships underlying PNUE variations. We found that LMA, mesophyll cell wall thickness (T_{cwm}), Rubisco N allocation fraction (P_R), and g_m together interpreted 83% of PNUE variations, 65% of which were explained by P_R and g_m. Paired-trait correlation analysis and path analysis indicated a weak correlation between PNUE and LMA, while the paired PNUE–T_{cwm} correlation was strong. There were positively interactive effects of P_R and g_m on PNUE. The effects of P_R on PNUE were species-dependent on g_m; that is, the P_R contribution on PNUE was massively greater in high-g_m species than that in low-g_m ones. The P_R was inversely proportional to T_{cwm} which was similar to the g_m–T_{cwm} relationship ($p < 0.01$). Additionally, g_m was positively regulated by chloroplast surface area exposed to intercellular airspace per unit leaf mass (S_c) ($p < 0.01$). Collectively, coordinated changes in P_R and g_m connecting T_{cwm} suggested the T_{cwm}-mediated complex physiology mechanisms controlling the PNUE across contrasting plant groups.

Keywords: photosynthetic nitrogen-use efficiency, nitrogen allocation, mesophyll conductance, cell wall thickness, leaf mass per area

Introduction

Photosynthetic nitrogen-use efficiency (PNUE) is defined as the ratio of light-saturated photosynthesis to leaf nitrogen content, being a core process of the leaf economics spectrum (LES) (Wright *et al*., 2005). Considerable variations in the PNUE economic trait were observed. There is a correlation between PNUE and LMA in spermatophyta: species with high LMA almost invariably have low PNUE (Reich *et al*., 1998; Wright *et al*., 2005; Onoda *et al*., 2017). The LMA, as a complex structural trait, cannot explain interspecific PNUE variation (Shipley *et al*., 2006; Warren and Adams, 2006; Hidaka and Kitayama, 2009; Onoda *et al*., 2017; Flexas and Carriquí, 2020; Luo *et al*., 2021). Given the ecological significance of the interspecific variations of PNUE with respect to relative growth rate and crop yield or for a sake of realistic ecosystem modeling (Poorter *et al*., 1990; Garnier *et al*., 1995; Reich *et al*., 1998; Oguchi *et al*., 2016; Yin *et al*., 2019), morpho-physiological mechanisms and interrelationships underlying the PNUE are attracting ever-increasing.

Previous studies suggested that variations in PNUE resulted from interactive mechanisms of several foliage physiological and anatomical traits (Hikosaka, 2004; Wright *et al*., 2005; Hikosaka, 2010; Onoda *et al*., 2017; Flexas and Carriquí, 2020). In particular, nitrogen allocation into photosynthetic apparatus and mesophyll conductance for internal CO_2 diffusion (g_m) were important. Experimental studies observed an inverse proportion phenomenon between LMA and the fraction of nitrogen allocated to photosynthetic proteins in spermatophyta. With increasing LMA in ten dicotyledonous species, photosynthetic N allocation fraction declined from 50% to 38%, with a large decline in the Rubisco N allocation fraction (P_R) (Poorter and Evans, 1998). Hikosaka *et al*. (1998) analyzed an annual herb and an evergreen tree, reporting a higher P_R of 23.2% in the low-LMA herb than the high-LMA tree. Similar results were also observed in other studies that the high-LMA species and genotypes had a smaller P_R (Warren and Adams, 2000; Ripullone *et al*., 2003; Onoda *et al*., 2004; Pons and Westbeek, 2004; Takashima *et al*., 2004; Onoda *et al*., 2017; Gvozdevaite *et al*., 2018; Lei *et al*., 2021a). A meta-analysis by Onoda *et al*. (2017) attributed the negative PNUE–LMA relationship to trade-off mechanisms between photosynthesis and structural persistence (hereinafter briefly called "pp trade-off opinion"), namely, species at the high-end of the LMA axis were prone to preserve a greater fraction of leaf nitrogen in structural tissues and thus had lower P_R and PNUE.

The PNUE variation from the low-end LMA axis to the high-end was related to increased N investments in structural tissue. Recently, a study quantifying a negative P_R–LMA relationship in spermatophyta has supported it (Luo *et al*., 2021).

An inevitable result of the construction cost for structural tissues is a reduction in g_m (Onoda *et al*., 2017; Flexas and Carriquí, 2020), with a declining tendency in g_m from the low-end of the LMA axis to the high-end in spermatophyta. In ferns and mosses, the observed PNUE variations were strongly associated with g_m (Tosens *et al*., 2016; Carriquí *et al*., 2019). Ferns and mosses with similar low LMA as seed plants had substantially lower PNUE as compared to the seed plants at the low-end of the LMA axis (Carriquí *et al*., 2015; Tosens *et al*., 2016), which indeed contradicted the negative PNUE–LMA pattern on which the LMA-based pp trade-off opinion was dependent. Contrasting to critical roles of g_m in PNUE in mosses and ferns, several studies in seed plants found that g_m did not contribute to PNUE variations in 11 evergreen tropical and temperate species that differed in LMA (Bahar *et al*., 2018) and in 26 wild and 31 domesticated cotton genotypes with large variations in LMA (Lei *et al*., 2021b). It suggested that the LMA-based pp trade-off framework in spermatophyta developed by Onoda *et al*. (2017) may have a limited capability of addressing the underpinnings of PNUE variations across land plant's phylogeny. Bryophytes and pteridophytes are important from an evolutionary point of view due to their pioneering positions in the land transition of photosynthetic life, and now attracting a considerable attention among researchers due to their great potential in biotechnology and bioindication (Preston and Hill, 1999; Popper and Fry, 2003; Wang *et al*., 2013; Gago *et al*., 2019; Flexas and Carriquí, 2020). However, the roles of LMA in PNUE variations, its correlations with g_m and P_R as well as g_m and P_R functioning mechanisms across major plant groups and phylogenetic interrelationships remain unclear.

The g_m is a highly complex trait with a strong sensitivity to leaf anatomy and biochemical traits mediating liquid phase diffusion (e.g., effective porosity of the cell wall-p_i, the CO_2 permeability of membranes, carbonic anhydrase activity) (Evans *et al*., 2009; Kaldenhoff, 2012; Tosens *et al*., 2012; Han *et al*., 2018; Gago *et al*., 2019; Carriquí *et al*., 2020; Evans, 2021; Flexas *et al*., 2021), which compound efforts to scale PNUE with g_m. Pleiotropic compensatory changes (e.g., one advantageous factor compensates for another drawback) may exert distinct roles when comparing PNUE in a few species or in species that occupy the same habitat in which resource

use strategies tend to converge (Evans *et al*., 2009; Lei et al., 2021b; Nadal *et al*., 2021). In order to advance the understanding of mechanisms regulating PNUE global variations, a comprehensive database was compiled, including leaf morphological, anatomical, and physiological traits of terrestrial C_3 species from bryophytes to angiosperm that were not considered in previous reviews (Hikosaka, 2004; Hikosaka, 2010; Onoda *et al*., 2017; Flexas *et al*., 2021). Data in C_4 species that have different photosynthetic mechanisms from the C_3 species were not the major concern in this study. Here, data analyses were made for the species within taxonomic groups (i.e., bryophytes, pteridophytes, gymnosperm, and angiosperm) and for all sampled species over an evolutionary time scale, respectively, because it is necessary to clarify the species range to which our conclusions were applicable. The data analysis campaign in the main body text was navigated by three key questions as follows:

(1) What is the evolutionary pattern of PNUE from bryophytes to angiosperm? Are PNUE variations across major taxonomic groups primarily associated with LMA?

(2) What are the interrelationships between P_R, g_m, and PNUE across major taxonomic groups?

(3) Are P_R and g_m variations across major taxonomic groups tightly associated with LMA? What are important morpho-anatomical factors in determining P_R and g_m?

Materials and Methods

Data collection

In this study, we constructed a global dataset of leaf morphological, anatomical, and physiological traits of non-stressed mature leaves of terrestrial C_3 species covering major plant groups and phylogeny. The dataset includes the photosynthetic organs with variable morphologies (e.g. phyllidia or thalli in mosses and lichen species). Leaf structural and anatomical traits included LMA and leaf thickness (T_{leaf}), chloroplast surface area exposed to intercellular airspace per unit leaf area (S_c), mesophyll surface area exposed to intercellular airspace per unit leaf area (S_m), cytoplasm thickness (T_{cyt}), mesophyll cell wall thickness (T_{cwm}), mesophyll thickness (T_{mes}), chloroplast thickness (T_{chl}), the fraction of intercellular air space (f_{ias}), the average distance between the chloroplast and the cell wall (cytoplasm thickness, L_{ct}). Physiological traits consisted of photosynthetic capacity at normal atmospheric CO_2 concentration and saturation light (A_{mass}, mass-based photosynthesis rate), leaf nitrogen content per leaf mass (N_{mass}), stomatal conductance to water vapor (g_s),

intercellular and chloroplastic CO_2 concentration (C_i and C_c, respectively), g_m, the maximum carboxylation rate (V_{cmax}), the maximum electron transport rate (J_{max}), stomatal limitation on photosynthesis (l_s), mesophyll limitation on photosynthesis (l_m), biochemical limitation on photosynthesis (l_b), and leaf temperature (L_{temp}). Papers that highlighted "mesophyll conductance" or "internal conductance" keywords archived by the Web of Science (https://www.webofscience.com) and the China National Knowledge Infrastructure (https://www.cnki.net) until 2022/05 were considered in this study. Trait measurements in most species including ferns and moss species in the field and/or outdoor conditions when their growth conditions were most favorable (i.e. with least environmental stress) were regarded as reliable for use. Measurements in shade-adapted leaves within plant canopies were not considered in the global database. The data collection campaign was challenged because these leaf traits were not presented together in papers. The number of available traits among papers varied greatly depending on their experimental objects and research purposes. If the traits that can only be measured were not available in papers, they were regarded as NA (not available) in the global database. Other traits that can be inferred/recalculated according to supporting information in papers were replenished to the global database to enrich data quantity, such as C_c, C_i, and P_R. The missing data in C_c was calculated from A_{area}, C_i, and g_m according to the Fick's law: $C_c = C_i - A/g_m$. The missing value in C_i was inferred from A_{area}, g_s, and ambient CO_2 concentration (C_a) using the Fick's law: $C_i = C_a - 1.56A/g_s$. It was worthy of note that bryophytes are the only group of plants that are entirely devoid of stomata. C_c values in bryophytes species were recalculated by the equation of $C_c = C_a - A/g_m$. C_a data available in papers were used, otherwise the global C_a of 380 ppm was applied. Except for the inferred trait values, other physiological and morpo-anatomical trait values were directly extracted from papers without any changes. Leaf trait data of the same species reported by different studies were averaged for use when environmental conditions sensed by the species were optimal to avoid any effect of environmental stress on analysis (Poorter *et al*., 2009; Poorter *et al*., 2011; Xing *et al*., 2021). In total, there were 1296 lines of data in 679 species (435 different species + 244 crop varieties), covering major life forms in land plants including bryophytes (57 lines in mosses and lichen species), pteridophytes (64 lines in ferns and fern allies species), gymnosperm (83 lines in needles and scales leaved species), and angiosperm (1092 lines in trees, shrubs, grass and crops).

The P_R was inferred by using two different methods: numerical calculation using V_{cmax} and N_{area} as shown by Niinemets and Tenhunen (1997), and chemical assay in Rubisco content. The dataset of P_R values obtained from the chemical assay offered by the study of Onoda *et al*. (2017) was solely limited to spermatophyte. Their P_R dataset was expanded by merging P_R numerical calculations to cover the four plant taxonomic groups. All leaf trait data in the global database were measured in sunlit leaves under relatively high incident radiation and ambient atmospheric CO_2 concentration at around 25°C. The P_R estimations by the numerical method were sensitive to measuring temperatures (Niinemets and Tenhunen, 1997). V_{cmax} and J_{max} measured at other leaf temperatures were converted to values at standard temperature 25°C using temperature response functions of V_{cmax} and J_{max} with activation energy (ΔH_a) at 63.0 kJ mol^{-1} according to Medlyn *et al.* (2002).

Data analysis

Because data types of some leaf traits were not a normal distribution, data of all traits were $\log_{10}$-transformed before correlation analysis, which was a common practice adopted in ecological studies (Wright *et al*., 2005; Carriquí *et al*., 2015; Tosens *et al*., 2016; Onoda *et al*., 2017; Carriquí *et al*., 2019). The standardized major axis slope (SMA, also known as reduced major axis slopes), a common practice seen in these studies, was applied to determine the strength of bivariate trait correlation. For paired traits with significant curvilinear relationship, rise to the maximum or decline to the minimum curve trajectory was predicted by the non-parametric regression model (locally weighted regression, Loess) following Xue *et al*. (2021) and Kurmangozhinov *et al*. (2020), aiming to clarify threshold at which trait strong coupling shifted to weak coupling. Indeed, it is the mass-based physiological traits such as A_{mass} that characterize the biochemical capacity of single cells and are the key players in the worldwide trade-off between the physiological and structural characteristics of foliage (Niinemets and Tenhunen, 1997; Wright *et al*., 2005; Tosens *et al*., 2016; Onoda *et al*., 2017). We found that the area-based trait analysis showed analogous results in correlation analysis as the mass-based trait expression. Hereinafter, the mass-based physiological traits were used for correlation analysis unless otherwise indicated. Before paired trait correlation analysis, we constructed a phylogenetic tree for all species using the megatree approach in the R package V.PHYLOMAKER and estimated the phylogenetic signals using the Pagel's λ

following Xing *et al*. (2021). There were 39 species failing to be bound to the constructed phylogenetic tree because they were not present in the plantlist database of the V.PHYLOMAKER package (package acquiring date: 2022/05/13). Of the 39 species, one was *Polistichium aculeatum* (pteridophyte) and the rest belonged to the bryophyte.

The paired-trait correlation analysis using the smatr package, Loess model application, and phylogenetic signal analysis using the V.PHYLOMAKER package was conducted in R 4.0.5 software (R Core Team, 2021). To explore how morpho-physiological traits influence PNUE variations, structural equation modeling (SEM) was applied (Shipley, 2004). The estimator to parameterize the SEMs was the maximum likelihood method. Appropriate SEM model fit was inspected by the comparative fit index (CFI, > 0.9), p-value, and the standard root mean squared residual (SRMR, < 0.08) (Shipley, 2004). The SEM analysis was conducted using the lavaan package (Rosseel, 2012) and visualized using the semPlot package in the R software.

The relative importance of P_R and g_m in relation to PNUE variations was quantified by the photosynthetic coordination theory. According to the biochemical photosynthesis model established by Farquhar *et al*. (1980), the photosynthetic rate is limited by either the Rubisco carboxylation rate at low Rubisco content and CO_2 concentrations (A_c) or the RuBP regeneration rate at relatively high CO_2 concentrations due to low electron transport rates (A_j). At a given leaf temperature, the A_c value is primarily determined by V_{cmax}, followed by C_c (Eqn 1). Different from the direct impacts of the P_R on photosynthesis, g_m effects on photosynthesis were realized through its impacts on C_c (Ethier & Livingston, 2004; Evans *et al*., 2009; Kaldenhoff, 2012; Tosens *et al*., 2012; Onoda *et al*., 2017; Gómez-Ocampo *et al*., 2021). The photosynthetic coordination theory originally proposed by von Caemmerer and Farquhar (1981) and further developed by Maire *et al*. (2012) in 31 individual C_3 species, Wang *et al*. (2017), Smith *et al*. (2019), and Harrison *et al*. (2021) in regional vegetation studies states that photosynthesis tends to be co-limited by electron transport and carboxylation under average environmental conditions, thus maximizing potential resource use for growth and reproduction. The photosynthetic coordination theory provides a quantitative approach to predicting P_R and g_m functioning effects on interspecific PNUE variations. The PNUE can be expressed with Eqn 3 that was inferred from Eqn 1 and Eqn 2 as follows:

$$A_{area} = (1-\frac{\Gamma^*}{C_c})A_c - R_d = (1-\frac{\Gamma^*}{C_c})\frac{V_{c\max}\cdot C_c}{C_c+K_m} - R_d \quad (1)$$

$$A_{area} / N_{area} = (1-\frac{\Gamma^*}{C_c})\frac{V_{c\max} / N_{area}}{1.0+K_m / C_c} - R_d / N_{area} \quad (2)$$

$$PNUE = (1-\frac{\Gamma^*}{C_c})\frac{6.25\cdot V_{cr}}{1+K_m / C_c}\cdot P_R - R_d / N_{area} \quad (3)$$

where V_{cr} is the maximum carboxylation rate per unit Rubisco protein (47.34 μmol CO_2 (g Rubisco)$^{-1}$ s^{-1} at 25°C) and 6.25 is the nitrogen content of Rubisco protein (Niinemets and Tenhunen, 1997; Luo *et al*., 2021); R_d is area-based dark respiration in the light; Γ* is chloroplast CO_2 compensation point, equal to 42.75 μmol mol^{-1} at 25°C. K_m is equal to $K_c/(1+O/K_o)$, where K_c and K_o are the Michaelis–Menten constants for CO_2 and O_2, respectively (Bernacchi *et al*., 2002). The PNUE simulations were generated considering a continuous series of P_R and C_c. We anticipated that impacts of g_m on PNUE changes were more obvious across contrasting plant groups with large differences in g_m than in several randomly selected species. Hence, the species in the global dataset were divided into two groups according to the g_m values: the high- and low-g_m species assembles. The high-g_m species assemble had g_m values ranging from 0.25 to 0.32 mol m^{-2} s^{-1}, and the low-g_m species assemble had g_m from 0.05 to 0.06 mol m^{-2} s^{-1}, corresponding to C_c at about 100 and 230 μmol mol^{-1} in leaves under current atmospheric CO_2 condition, respectively. The PNUE and P_R measurements together with g_m and C_c measurements (i.e., trait values directly extracted/inferred from papers) in the two species assembles were applied to cross-validate the PNUE theoretical analysis. Variations in predicted PNUE were assumed to be not affected by the intercept R_d/N_{area}.

Results

The evolutionary pattern of PNUE and its relationship with LMA

The LMA, PNUE, A_{mass}, N_m, V_{cmax}, J_{max}, P_R, g_m, DeltaC, and T_{cwm} exhibited significant phylogenetic signals (Table S1). Firstly, we mapped the LMA phylogenetic pattern and its relationship with PNUE, A_{mass}, and N_m because LMA was considered a critical factor influencing the PNUE economic trait (Hikosaka, 2004; Wright *et al*., 2005; Onoda *et al*., 2017). The mean of LMA cluster data slightly increased from bryophytes to pteridophytes (TukeyHSD, p = 0.07) (Fig. 1a). No significant differences in mean LMA were observed between pteridophytes and angiosperm (p = 0.27, Fig. 1a). The mean LMA in gymnosperm was significantly

304 higher than in the other three phyla ($p < 0.01$). The ANOVA results in mean PNUE
305 showed significant differences among the four phyla (Fig. 1b), with the highest PNUE
306 found in angiosperm ($p < 0.05$) and similar PNUE values among the other three phyla
307 ($p > 0.1$). Significantly lower PNUE was evident in bryophytes at the same LMA as
308 seed plants, and pteridophyte had slightly lower PNUE (Fig. 1c). The LES SMA
309 regression (SMA model fit all data in the LES) had a low r^2 at 0.1, due to a significant
310 deviation of bryophytes data from the LES SMA regression line (Fig. 1c, SMA
311 ANOVA in intercept: $p < 0.01$). Improved performance in the LES SMA regression
312 for A_{mass}–LMA was evident ($r^2 = 0.33$), whereas all A_{mass} values in bryophytes
313 significantly deviated from the LES SMA regression line primarily due to large
314 differences in intercept (Fig. 1d, SMA ANOVA in intercept: $p < 0.01$). For the N_m–
315 LMA relationship, the LES SMA regression line and the phylum SMA regression
316 lines (SMA model fit data of each phylum) were close to each other (Fig. 1e),
317 showing significantly higher $r^2 = 0.53$. It was suggested that PNUE variations through
318 plant phylogeny were weakly associated with LMA primarily due to large
319 discrepancies in slope and intercept of the A_{mass}–LMA relationship among major
320 taxonomic groups.

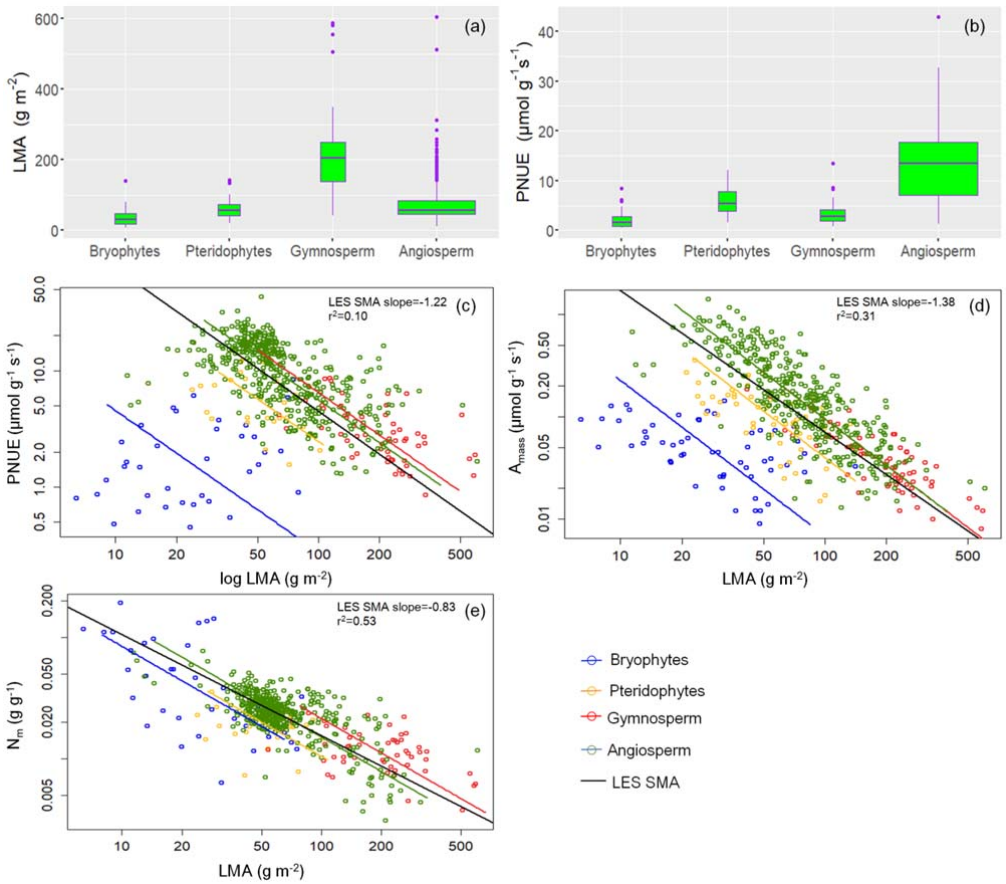

Fig. 1. The phylogenetic patterns of leaf mass per area (LMA, a) and photosynthetic N-use efficiency (PNUE, b), and paired-trait relationships between PNUE, mass-based photosynthesis (A_{mass}), leaf nitrogen content per leaf mass (N_m), and LMA. (c) PNUE–LMA, (d) A_{mass}–LMA, (e) N_m–LMA. The black line was the regression of standard major analysis (SMA) fit to all data in the leaf economics spectrum (LES) and the other lines were SMA regressions fit to all data of each phylum. The r^2 and slope values were annotated for the LES SMA regression. The boxes were drawn with widths proportional to the square-roots of the number of observations in the phyla. The same symbol legends for bryophytes, pteridophytes, gymnosperm, and angiosperm as Fig. 1 were used in other figures unless otherwise indicated.

Effects of photosynthetic nitrogen allocation and g_m on photosynthesis and PNUE variations

No significant correlation for PNUE–N_m was observed (LES SMA regression $r^2 = 0.002$, $p = 0.32$), while the LES SMA fit for PNUE–A_{mass} had r^2 as high as 0.58 (Fig. S1), suggesting that PNUE changing patterns along the LMA axis were primarily shaped by A_{mass}. Hence, quantitative relationships between key physiological traits and A_{mass} were explored in this paragraph. A positive LES SMA regression line for the A_{mass}–V_{cmax} relationship had $r^2 = 0.68$, which overlapped the four phylum regression lines well (Fig. 2a, SMA ANOVA in slope: $p = 0.07$). A closer correlation

for the LES SMA regression fit to A_{mass}–g_m was evident with r^2 at 0.74, without showing significant differences against phylum regression lines (Fig. 2b, SMA ANOVA in slope: p = 0.9). The V_{cmax} was tightly related to J_{max} with r^2 as high as 0.89 (Fig. 2c), close to four phylum regression lines (SMA ANOVA in slope: p = 0.04). The g_m and V_{cmax} relationship featured relatively weaker correlation strength than that for V_{cmax}–J_{max} (r^2 = 0.5, Fig. 2d).

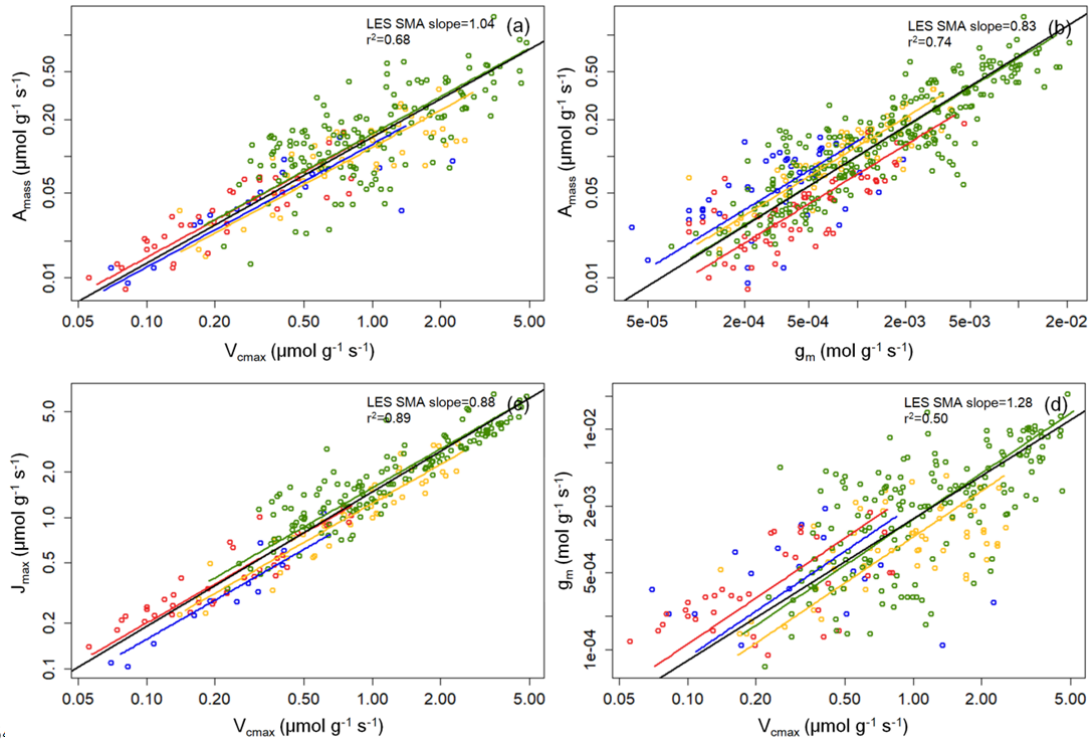

Fig. 2. Paired-trait relationships between the mass-based photosynthesis (A_{mass}), the mass-based maximum carboxylation rate (V_{cmax}), the mass-based mesophyll conductance (g_m), and the mass-based maximum electron transport rate (J_{max}). (a) A_{mass}–V_{cmax}, (b) A_{mass}–g_m, (c) V_{cmax}–J_{max}, and (d) g_m–V_{cmax}. The black line was the regression of standard major analysis (SMA) fit to all data in the leaf economics spectrum (LES) and the other lines were SMA regressions fit to all data of each phylum. The r^2 and slope values were annotated for the LES SMA regression.

The A_{mass} was strongly regulated by V_{cmax} which was in turn related to P_R (LES SMA r^2 = 0.62). Onoda *et al*. (2017) suggested that DeltaC may be an important factor influencing PNUE variations. Hence, PNUE correlations with P_R, g_m, and DeltaC were quantified in Fig. 3. We found strong correlation strength between PNUE and P_R across the four phyla (r^2 = 0.45, Fig. 3a). The PNUE–g_m correlation had a higher r^2 (0.52, Fig. 3c) than that with P_R. Path analysis indicated that the two traits explained about 65% of PNUE variations. There was no obvious correlation between PNUE and DeltaC across the four phyla (r^2 = 0.04, Fig. 3c). The r^2 value was

relatively lower for the P_R–g_m relationship (r^2 = 0.20, Fig. 3d), suggesting a weak correlation between them.

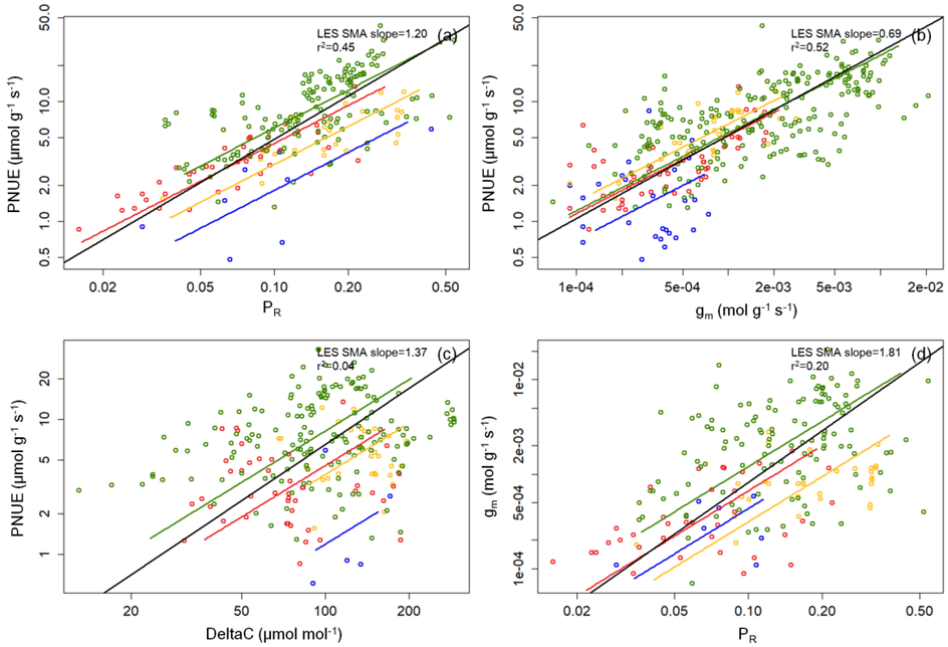

Fig. 3. Paired-trait relationships between the photosynthetic N-use efficiency (PNUE), allocation fraction of leaf nitrogen to Rubisco (P_R), mass-based mesophyll conductance (g_m), internal CO_2 drawdown (DeltaC). (a) PNUE–P_R, (b) PNUE–g_m, (c) PNUE–DeltaC, (d) P_R–g_m. The black line was the regression of standard major analysis (SMA) fit to all data in the leaf economics spectrum (LES) and the other lines were SMA regressions fit to all data of each phylum. The r^2 and slope values were annotated for the LES SMA regression.

Clarifying the relative importance of P_R and g_m in determining PNUE was achieved by applying Eqn 3. The PNUE predictions corresponded to observations well at the low- and high-g_m assembles (Fig. 4a). A close correspondence between PNUE predictions and observations was also observed in most sampled species (Fig. S2). In the high-g_m assemble (0.25–0.32 mol m^{-2} s^{-1}), the slope of the PNUE–P_R relationship was 57.58, and it was 20.52 for the low-g_m assemble (0.05–0.06 mol m^{-2} s^{-1}). It suggested that for species with high g_m, a 0.1-unit increase in P_R contributed to a 5.8-unit increase in PNUE, whereas the increment of PNUE was only 2.1-unit in low-g_m species. An exponential decay tendency in l_m-l_b with g_m was observed in all sampled species (Fig. 4b). The l_m overweighed l_b in species with low g_m < 0.001 mol g^{-1} s^{-1} (ca. 0.08 mol m^{-2} s^{-1}), suggesting stronger mesophyll limitation on photosynthesis; *vice verse*, stronger biochemical limitation on photosynthesis was evident in species with high g_m > 0.001 mol g^{-1} s^{-1}. These results suggested stronger

limitation by g_m on PNUE for species with low g_m and stronger limitation by P_R on PNUE in species with high g_m.

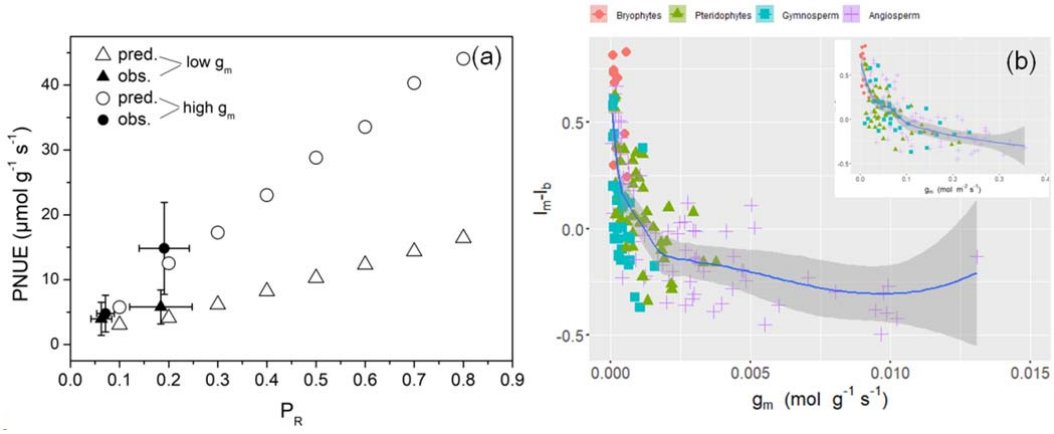

Fig. 4. Model simulations and observations of photosynthetic N-use efficiency (PNUE) at a continuous series of Rubisco nitrogen allocation fraction (P_R) and at two assembles of mesophyll conductance (g_m): high and low ranges (circles and triangles, respectively) in subplot a. Subplot b showed the relationship between l_m-l_b and mass- and area-based g_m. The high-g_m assemble had g_m range from 0.25 to 0.32 mol m^{-2} s^{-1} and 0.05–0.06 mol m^{-2} s^{-1} in the low-g_m assemble, corresponding to chloroplast CO_2 concentration (C_c) at about 100 and 230 μmol mol^{-1} under current atmospheric CO_2 condition, respectively. pred.: predictions; obs.: observations; l_m-l_b: the difference between mesophyll conductance limitation and biochemical limitation.

Relationships between morpho-anatomical traits and P_R and g_m

Relationships between morpho-anatomical traits and P_R and g_m are shown in Fig. 5. The P_R had a weak correlation with LMA across the four phyla (r^2 = 0.19, Fig. 5a) and the weak correlation was also observed for g_m and LMA (r^2 = 0.24, Fig. 5b) Statistical results in comparison between Onoda P_R dataset and ours in spermatophyte showed no significant differences in SMA slope and intercept (p = 0.1, Fig. S3), suggesting that incorporation of P_R numerical calculations into Onoda P_R dataset did not bring systematic biases in trait correlation analysis, and our global P_R dataset was reliable. For g_m and T_{cwm}, a consistent relationship with high correlation strength was observed across the four phyla (r^2 = 0.44, Fig. 5c). The g_m in four phyla tended to converge towards the Loess regression line (insert in Fig. 5c). A rapid decline in g_m with T_{cwm} was seen, and g_m tended to level off at higher T_{cwm}. A strong correlation was observed between g_m and the mass-based S_c (r^2 = 0.66, Fig. 5d). Other anatomical traits did not show a significant correlation with g_m (r^2 < 0.1, Figs. S4a–f). The P_R was inversely proportional to T_{cwm} with a medium r^2 = 0.30 (Fig. 5e). The DeltaC increased with increasing T_{cwm}, while their correlation strength was much weaker (r^2

= 0.14, Fig. 5f), suggesting marginal effects of T_{cwm} on the CO_2 drawdown from intercellular airspaces to carboxylation sites inside chloroplasts.

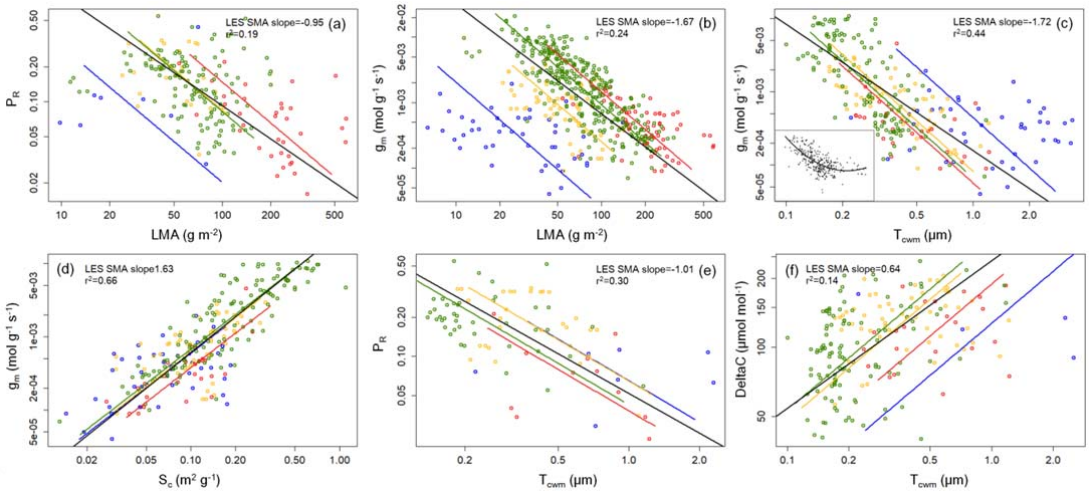

Fig. 5. Paired-trait correlations between allocation fraction of leaf nitrogen to Rubisco (P_R), leaf mass per area (LMA), mesophyll conductance (g_m), mesophyll cell wall thickness (T_{cwm}), chloroplast surface exposed to intercellular airspace area per unit leaf mass (S_c), internal CO_2 drawdown (DeltaC). (a) P_R–LMA, (b) g_m–LMA, (c) g_m–T_{cwm}, (d) g_m–S_c, (e) P_R–T_{cwm}, (f) DeltaC–T_{cwm}. The black line was the regression of standard major analysis (SMA) fit to all data in the leaf economics spectrum (LES) and the other lines were SMA regressions fit to all data of each phylum. The r^2 and slope values were annotated for the LES SMA regression. The insert in subplot c showed the Loess model fit to the g_m–T_{cwm} correlation.

Path analysis for leaf morpho-anatomical and physiological traits and PNUE

Path analysis for the SEM fit indicated that the seven traits g_m, P_R, LMA, T_{cwm}, mass-based S_c, C_i, and C_c together explained 88% of PNUE variations, and 65% of PNUE variations were interpreted by P_R and g_m (CFI = 1.0, SRMR = 0.02, p = 0.001, Fig. 6a). The traits used for path analysis was chosen primarily according to the aforementioned paired-trait correlation analysis and Eqn 3. The absolute value of path coefficient (Q) for T_{cwm}–g_m was 0.84, which was higher by 13.5% than that for LMA–g_m. A higher Q value of 27.5% was found in the T_{cwm}–P_R as compared to the LMA–P_R. The Q values for P_R–C_i or P_R–C_c were less than 0.3, suggesting low impacts of leaf internal CO_2 concentration on P_R changes across species. The P_R and g_m had direct and substantial impacts on PNUE ($Q > 0.45$), while direct impacts on PNUE by T_{cwm} and LMA were much weaker (Q = 0.1 and 0.25, respectively). Paired-trait correlation for PNUE-T_{cwm} was drawn in Fig. 6b in order to show their r^2 value. The PNUE was negatively proportional to T_{cwm} with r^2 as high as 0.61, which was higher by five-fold than the PNUE–LMA relationship shown in Fig. 1c. Results suggested

that P_R and g_m variations across the four phyla and through plant phylogeny were primarily related to T_{cwm}. Impacts of T_{cwm} on PNUE were achieved through its controls on P_R and g_m.

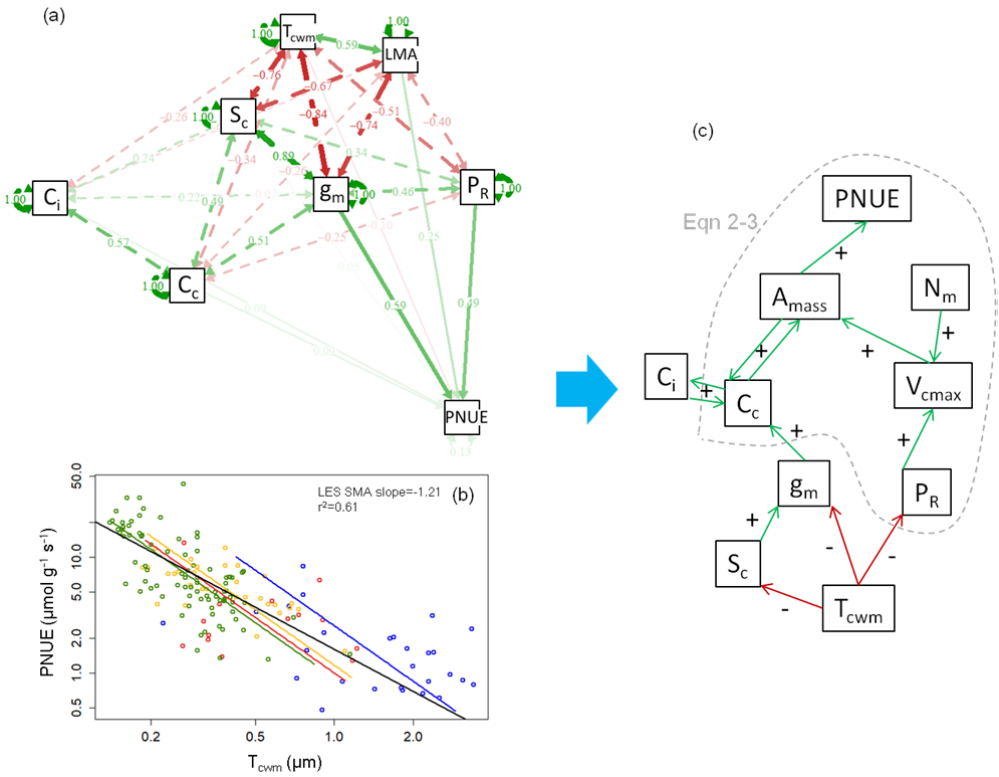

Fig. 6. Subplot a indicated the circle layout of the path diagram that represents relationships and the causal direction between photosynthetic-N use efficiency (PNUE) and allocation fraction of leaf nitrogen to Rubisco (P_R), leaf mass per area (LMA), mass-based mesophyll conductance (g_m), mesophyll cell wall thickness (T_{cwm}), chloroplast surface area exposed to intercellular airspace per unit leaf mass (S_c), and leaf intercellular and chloroplastic CO_2 concentration (C_i and C_c, respectively). The arrow and value between each trait and PNUE indicate the path coefficient. Subplot b illustrated the paired-trait relationship between PNUE and T_{cwm}. The black line was the regression of standard major analysis (SMA) fit to all data in the leaf economics spectrum (LES) and the other lines were SMA regressions fit to all data of each phylum. The r^2 and slope values were annotated for the LES SMA regression. Subplot c presented the structural diagram about T_{cwm}-mediated physiological mechanisms controlling PNUE variations. Intercorrelationships between PNUE and leaf traits embedded by the gray dashed circle in subplot c were deduced according to Eqn 2-3. The "+" and "-" signs reflected positive and negative relations, respectively.

Discussion

Thematic results with casual correlations between leaf traits and PNUE were visualized in Fig. 6c. According to Eqn 2-3, A_{mass} was determined by C_c and V_{cmax}, which in turn were primarily related to C_i and g_m, and P_R and N_m, respectively. PNUE

469 was explicitly expressed by a division value of A_{mass} and N_m in the global database.
470 Increment of N_m could contribute to V_{cmax} and then A_{mass}, while its contributions to
471 PNUE were not significant (Fig. S1). In fact, A_{mass} and N_m was positively related with
472 each other across species (LES SMA $r^2 = 0.34$). Hence, improvement in A_{mass} per unit
473 of leaf nitrogen through C_c and P_R was of high priority for the achievement of high
474 PNUE (Hikosaka *et al*., 2002; Warren and Adams, 2006; Hikosaka, 2010). Previous
475 studies reported that C_i varied slightly across species grown under non-stress
476 conditions under current atmospheric CO_2 conditions (von Caemmerer and Farquhar,
477 1981; Evans *et al*., 2009). The coefficient of variation (CV) for C_i in the global
478 database was 0.15, which accounted for about a half of the CV of C_c. It might be
479 reasonable to infer the critical roles of g_m rather than g_s in the determination of C_c
480 across non-stressed plant species (Ethier and Livingston, 2004; Evans *et al*., 2009;
481 Tosens *et al*., 2012; Onoda *et al*., 2017). Cell walls (CWs) have a well recognized
482 importance in plant physiology and biotechnology, and recent reviews suggested that
483 T_{cwm} can be crucial in regulating photosynthesis along the terrestrial plant's
484 phylogeny (Flexas and Carriquí, 2020; Flexas *et al*., 2021). In the paragraphs that
485 followed, T_{cwm}-mediated complex physiological mechanisms controlling PNUE
486 variations through plant phylogeny were discussed.

487 The P_R and g_m were considered two important factors underlying PNUE
488 variations in seed plants (Hikosaka, 2004; Onoda *et al*., 2017). Our results
489 documented the synergetic effects of the two variables on PNUE variations across
490 plant phylogeny, namely an increase in one of the two factors could contribute to the
491 improvement of PNUE. However, the extent of the synergetic effect of P_R was
492 determined by g_m. Increasing P_R contributed to a slight improvement in PNUE in
493 species with low g_m, whereas a double increment in PNUE was achieved in high-g_m
494 species (Fig. 4a), primarily due to positive effects of g_m on C_c, the substrate
495 concentration for Rubisco carboxylation process. Variation in the g_m–photosynthesis
496 relationship contributes to variation in PNUE (Warren and Adams, 2006).
497 Photosynthesis was strongly limited by g_m in species with low $g_m < 0.001$ mol g^{-1} s^{-1}
498 (Fig. 4b); *vice versa*, the biochemical limitation was a major factor constraining
499 photosynthesis in high-g_m species. The g_m threshold where the relative importance of
500 P_R and g_m in determining PNUE shifted maybe at 0.001 mol g^{-1} s^{-1}, corresponding to
501 area-based g_m from 0.05 to 0.1 mol m^{-2} s^{-1}. Covariations in A_{mass}, g_m, and Rubisco
502 content in hundreds of rice varieties were evaluated by Xiong and Flexas (2018),

finding lower g_m limitation and stronger Rubisco limitation in modern varieties. Under high-resource agricultural environments, PNUE improvement in modern varieties would be further facilitated by the improvement of Rubisco carboxylation capacity. It suggested that Rubisco carboxylation capacity was critical in shaping PNUE in high-g_m plants. Collectively, PNUE variations across major plant groups were strongly characterized by P_R and g_m wherein their interactive effects varied depending on g_m.

The g_m is a composite conductance of the CO_2 diffusion pathway between the substomatal cavities and the sites of carboxylation within chloroplasts. Previous studies highlighted the importance of cell wall composition (Ellsworth *et al*., 2018; Carriquí *et al*., 2020; Roig-Oliver *et al*., 2021), cell wall porosity (Evans *et al*., 2009), cell wall thickness (Carriquí *et al*., 2015, 2019, 2021; Flexas *et al*., 2021), chloroplast distribution, in particular the S_c (Carriquí *et al*., 2015, 2019; Tosens *et al*., 2016; Han *et al*., 2018; Du *et al*., 2019; Ren *et al*., 2019; Nadal *et al*., 2021), in determining g_m. Our results suggested that strong and positive correlation between g_m and S_c, while significantly negative relationship between g_m and T_{cwm} across major plant groups and through phylogeny (Figs. 5c and d; Fig. 6a). There is an exponential decay tendency in g_m with increasing T_{cwm}, and the low g_m value tended to level off at greater T_{cwm} (Fig. S5), implying that species with thicker cell walls may have the same g_m as compared to those with relatively thin cell walls. As reported in resurrection plants with thick T_{cwm} by Nadal *et al*. (2021), greater S_c could compensate for thick cell wall limitation to obtain relatively high g_m. It explained scattered g_m values at given T_{cwm} shown in Fig. 5c.

A negative P_R–LMA relationship in regional vegetation was reported by Luo *et al*. (2021). In line with their reports, the P_R was inversely scaled with LMA (Fig. 5a), and the relationship was analogous to the g_m–T_{cwm} relationship. There is a progressive phylogenetic trend associated with LMA and T_{cwm} in spermatophyta: from low LMA and thin T_{cwm} in angiosperms to high LMA and great T_{cwm} in gymnosperm (Onoda *et al*., 2017; Flexas *et al*., 2021; Xing *et al*., 2021), while an exception occurred in mosses and ferns that have low LMA (Tosens *et al*., 2016; Carriquí *et al*., 2019). Interestingly, a consistent phylogenetic trend regarding T_{cwm} from bryophytes to angiosperm was reported in the study of Gago *et al*. (2019) and in Fig. S6 in our study: from very large T_{cwm} in bryophytes to very low T_{cwm} in angiosperms. Higher correlation strength was indeed achieved when scaling g_m with T_{cwm} as compared to

that for g_m–LMA (Figs. 5b and c and Fig. 6a). The log-transformed g_m–T_{cwm} relationship exhibited more convergent characteristics in g_m changes with T_{cwm} (i.e., g_m coming closer together at given T_{cwm}). It suggested that the P_R–T_{cwm} relationship was likely synonymous with the exponential decay correlation of P_R–LMA, or at least it should be. Theoretical predictions by Evans *et al.* (2009) suggested that other elements in the mesophyll CO_2 diffusion pathway of the liquid phase could co-vary with T_{cwm}, such as a decline in Rubisco per unit of exposed chloroplast surface area and thinner chloroplast with increasing T_{cwm}. If the P_R, which was proportional to photosynthesis, did not decrease with increases in T_{cwm}, then the CO_2 drawdown "DeltaC" would have been much greater than observations. If the g_m decreased by ten folds due to increasing T_{cwm} from 0.2 to 0.5 μm (e.g., the g_m decline from 0.004 to 0.0004 mol g^{-1} s^{-1}), then cell wall thickness 0.5 μm would increase CO_2 drawdown by more than five folds, and strong correlation between DeltaC and T_{cwm} would therefore be observed. However, this expectation contradicts the fact that the actual increment of CO_2 drawdown was limited to 50% (Fig. 5f). The net result of the decline in P_R with T_{cwm} was to balance the increase in mesophyll resistance so that the CO_2 drawdown was only weakly proportional to T_{cwm} (Fig. 5f). The theoretical prediction regarding the T_{cwm}–biochemical capacity offset mechanisms in the study of Evans *et al*. (2009) was supported by experimental results in this study, i.e., a significantly negative correlation between T_{cwm} and P_R (Fig. 5e and Fig. 6a). In our study, the observed significance of T_{cwm}–P_R negative correlation across major plant groups was aligned with the founding in seed plants in the study of Onoda *et al*. (2017). However, the predicted inverse correlation between chloroplast thickness and T_{cwm} was not observed (Fig. S7). One of the distinctive differences in leaf anatomy among bryophytes, ferns, and spermatophytes was the thickness of photosynthetic tissues (Han *et al*., 2018; Carriquí *et al*., 2019). The T_{cwm}-induced decline in P_R may result in the decline of chloroplast amount per leaf mass. An open question arose regarding whether the response pattern of P_R to T_{cwm} was exclusively independent or dependent causality due to g_m changes. The possibility of g_m effects on the observed P_R–T_{cwm} response pattern could be excluded because no strong intercorrelation was observed for either P_R–g_m relationship (Fig. 3d) or V_{cmax}–C_c relationship (Fig. S8). Concerning the generality of significant correlations for P_R–T_{cwm} and g_m–T_{cwm} in the global database, it suggested that T_{cwm} was the critical factor controlling evolutionary changes of PNUE from bryophytes to angiosperm.

Concluding remarks

The most important results derived from the large matrix of plant leaf traits were understandings of complex morpho-physiological mechanisms underlying PNUE variations. Theoretical predictions and correlation analysis suggested that P_R and g_m concurrently contributed to PNUE variations among species, whereas P_R contributions on PNUE were strongly constrained by g_m: improvement of PNUE in high-g_m species due to increasing P_R was much higher than that in low-g_m species. The P_R and g_m were inversely proportional to T_{cwm} across plant phylogeny such that internal CO_2 drawdown along T_{cwm} did not increase significantly. Meanwhile, g_m was positively regulated by S_c. Path analysis suggested a weak correlation between PNUE and T_{cwm}. In fact, T_{cwm} is critical in determining the evolutional direction of PNUE through its controls on g_m and P_R.

Understanding the complex mechanisms underlying the PNUE has two major importance. First, canopy leaf PNUE emerged as a key target in crop resource use efficiency initiatives to ensure food security and environmental quality (Tester and Langridge, 2010; Fan *et al.*, 2011). They suggested that in the face of global environmental change, new crop varieties will need to be more efficient in their use of nitrogenous fertilizers. Modification of cell wall thickness to improve crop PNUE may be a promising direction because changing cell wall thickness would bring coordinated changes in biochemical activity and mesophyll conductance to maximize PNUE. Secondly, the predictive power of process-based vegetation models is importantly determined by the correct estimation of PNUE.

Acknowledgments

This work was supported by the National Natural Science Foundation of China (32001129), the Research and Promotion Project of Gansu Agricultural New Technology and Equipment (RWS-NYSTZZ202102), and Estonian Research Council (PUT 1473).

Author contributions:

Conceptualization: DDL, WX

Methodology: WX

Investigation: DDL, XS, WX

Visualization: DDL, XS, WX

Supervision: WX

Writing—original draft: DDL, XS, WX

Writing—review & editing: MC, DLX, TT, YCX, WX

Competing interests: Authors declare that they have no competing interests.

Data and materials availability: All data are available in the supplementary materials.

References

Bahar N H A, Hayes L, Scafaro A P, Atkin O K, Evans J R. 2018. Mesophyll conductance does not contribute to greater photosynthetic rate per unit nitrogen in temperate compared with tropical evergreen wet-forest tree leaves. New Phytologist 218, 492-505.

Bernacchi C J, Portis A R, Nakano H, von Caemmerer S, Long S P. 2002. Temperature response of mesophyll conductance. Implications for the determination of Rubisco enzyme kinetics and for limitations to photosynthesis in vivo. Plant Physiology 130, 1992-1998.

Carriquí M, Cabrera H M, Conesa M À, Coopman R E, Douthe C, Gago J, Gallé A, Galmés J, Ribas-Carbo M, Tomás M et al. 2015. Diffusional limitations explain the lower photosynthetic capacity of ferns as compared with angiosperms in a common garden study. Plant, Cell & Environment 38, 448-460.

Carriquí M, Roig-Oliver M, Brodribb T J, Coopman R, Gill W, Mark K, Niinemets Ü, Perera-Castro A V, Ribas-Carbó M, Sack L et al. 2019. Anatomical constraints to nonstomatal diffusion conductance and photosynthesis in lycophytes and bryophytes. New Phytologist 222, 1256-1270.

Carriquí M, Nadal M, Clemente-Moreno MJ, Gago J, Miedes E, Flexas J. 2020. Cell wall composition strongly influences mesophyll conductance in gymnosperms. The Plant Journal 103, 1372-1385.

Carriquí M, Nadal M, Flexas J. 2021. Acclimation of mesophyll conductance and anatomy to light during leaf aging in *Arabidopsis thaliana*. Physiologia Plantarum 172, 1894-1907.

638 Du Q J, Liu T, Jiao X, Song X M, Zhang J Y, Li J M. 2019. Leaf anatomical
639 adaptations have central roles in photosynthetic acclimation to humidity. Journal
640 of Experimental Botany 70, 4949-4961.
641 Ellsworth P V, Ellsworth P Z, Koteyeva N K, Cousins A B. 2018. Cell wall properties
642 in *Oryza sativa* influence mesophyll CO_2 conductance. New Phytologist 219, 66-
643 76.
644 Ethier G J, Livingston N J. 2004. On the need to incorporate sensitivity to CO_2
645 transfer conductance into the Farquhar–von Caemmerer–Berry leaf
646 photosynthesis model. Plant, Cell & Environment 27, 137-153.
647 Evans J R, Kaldenhoff R, Genty B, Terashima I. 2009. Resistances along the CO_2
648 diffusion pathway inside leaves. Journal of Experimental Botany 60, 2235-2248.
649 Evans J R. 2021. Mesophyll conductance: walls, membranes and spatial complexity.
650 New Phytologist 229, 1864-1876.
651 Fan M, Shen J, Yuan L, Jiang R, Chen X, Davies W J, Zhang F. 2011. Improving
652 crop productivity and resource use efficiency to ensure food security and
653 environmental quality in China. Journal of Experimental Botany 63, 13-24.
654 Farquhar G D, von Caemmerer S, Ball J A. 1980. A biochemical model of
655 photosynthetic CO_2 assimilation in leaves of C_3 species. Planta 149, 78-90.
656 Flexas J, Carriquí M. 2020. Photosynthesis and photosynthetic efficiencies along the
657 terrestrial plant's phylogeny: lessons for improving crop photosynthesis. The
658 Plant Journal 101, 964-978.
659 Flexas J, Clemente-Moreno M J, Bota J, Brodribb T J, Gago J, Mizokami Y, Nadal
660 M, Perera-Castro A V, Roig-Oliver M, Sugiura D et al. 2021. Cell wall thickness
661 and composition are involved in photosynthetic limitation. Journal of
662 Experimental Botany 72, 3971-3986.
663 Gago J, Carriquí M, Nadal M, Clemente-Moreno M J, Coopman R E, Fernie A R,
664 Flexas J. 2019. Photosynthesis optimized across land plant phylogeny. Trends in
665 Plant Science 24, 947-958.
666 Garnier E, Gobin O, Poorter H. 1995. Nitrogen productivity depends on
667 photosynthetic nitrogen use efficiency and on nitrogen allocation within the
668 plant. Annals of Botany 76, 667-672.
669 Gómez-Ocampo G, Ploschuk E L, Mantese A, Crocco C D, Botto J F. 2021. BBX21
670 reduces abscisic acid sensitivity, mesophyll conductance and chloroplast electron

transport capacity to increase photosynthesis and water use efficiency in potato plants cultivated under moderated drought. The Plant Journal 108, 1131-1144.

Gvozdevaite A, Oliveras I, Domingues T F, Peprah T, Boakye M, Afriyie L, da Silva Peixoto K, de Farias J, Almeida de Oliveira E, Almeida Farias et al. 2018. Leaf-level photosynthetic capacity dynamics in relation to soil and foliar nutrients along forest–savanna boundaries in Ghana and Brazil. Tree Physiology 38, 1912-1925.

Han J M, Lei Z Y, Flexas J, Zhang Y J, Carriqui, Zhang W F, Zhang Y L. 2018. Mesophyll conductance in cotton bracts: anatomically determined internal CO_2 diffusion constraints on photosynthesis. Journal of Experimental Botany 69, 5433-5443.

Harrison S P, Cramer W, Franklin O, Prentice I C, Wang H, Brännström Å, de Boer H, Dieckmann U, Joshi J, Keenan T F, Lavergne A. 2021. Eco-evolutionary optimality as a means to improve vegetation and land-surface models. New Phytologist 231, 2125-2141.

Hidaka A, Kitayama K. 2009. Divergent patterns of photosynthetic phosphorus-use efficiency versus nitrogen-use efficiency of tree leaves along nutrient-availability gradients. Journal of Ecology 97, 984-991.

Hikosaka K, Hanba Y T, Hirose T, Terashima I. 1998. Photosynthetic nitrogen-use efficiency in leaves of woody and herbaceous species. Functional Ecology 12, 896-905.

Hikosaka K, Nagamatsu D, Ishii H S, Hirose T. 2002. Photosynthesis-nitrogen relationships in species at different altitudes on Mount Kinabalu, Malaysia. Ecological Research 17, 305-313.

Hikosaka K. 2004. Interspecific difference in the photosynthesis-nitrogen relationship: patterns, physiological causes, and ecological importance. Journal of Plant Research 117, 481-494.

Hikosaka K. 2010. Mechanisms underlying interspecific variation in photosynthetic capacity across wild plant species. Plant Biotechnology 27, 223-229.

Kaldenhoff R. 2012. Mechanisms underlying CO_2 diffusion in leaves. Current Opinion in Plant Biology 15, 276-281.

Kurmangozhinov A, Xue W, Li X, Zeng F, Sabit R, Tusun T. 2020. High biomass production with abundant leaf litterfall is critical to ameliorating soil quality and

704 productivity in reclaimed sandy desertification land. Journal of Environmental
705 Management 263, 110373.
706 Lei Z Y, Wang H, Wright I J, Zhu X-G, Niinemets Ü, Li Z-L, Sun D S, Dong N,
707 Zhang W F, Zhou Z L et al. 2021a. Enhanced photosynthetic nitrogen use
708 efficiency and increased nitrogen allocation to photosynthetic machinery under
709 cotton domestication. Photosynthesis Research 150, 239-250.
710 Lei Z, Liu F, Wright I J, Carriquí M, Niinemets Ü, Han J, Jia M, Atwell B J, Cai X,
711 Zhang W et al. 2021b. Comparisons of photosynthetic and anatomical traits
712 between wild and domesticated cotton. Journal of Experimental Botany 73, 873-
713 885.
714 Luo X, Keenan T F, Chen J M, Croft H, Colin Prentice I, Smith N G, Walker A P,
715 Wang H, Wang R, Xu C et al. 2021. Global variation in the fraction of leaf
716 nitrogen allocated to photosynthesis. Nature Communications 12.
717 Maire V, Martre P, Kattge J, Gastal F, Esser G, Fontaine S, Soussana J F. 2012. The
718 coordination of leaf photosynthesis links C and N fluxes in C_3 plant species. Plos
719 One 7.
720 Medlyn B E, Dreyer E, Ellsworth D, Forstreuter M, Harley P C, Kirschbaum M U F,
721 Le Roux X, Montpied P, Strassemeyer J, Walcroft A. 2002. Temperature
722 response of parameters of a biochemically based model of photosynthesis. II. A
723 review of experimental data. Plant, Cell & Environment 25, 1167-1179.
724 Nadal M, Perera-Castro A V, Gulías J, Farrant J M, Flexas J. 2021. Resurrection
725 plants optimize photosynthesis despite very thick cell walls by means of
726 chloroplast distribution. Journal of Experimental Botany 72, 2600-2610.
727 Niinemets Ü, Tenhunen J D. 1997. A model separating leaf structural and
728 physiological effects on carbon gain along light gradients for the shade-tolerant
729 species Acer saccharum. Plant, Cell & Environment 20, 845-866.
730 Oguchi R, Ozaki H, Hanada K, Hikosaka K. 2016. Which plant trait explains the
731 variations in relative growth rate and its response to elevated carbon dioxide
732 concentration among Arabidopsis thaliana ecotypes derived from a variety of
733 habitats? Oecologia 180, 865-876.
734 Onoda Y, Hikosaka K, Hirose T. 2004. Allocation of nitrogen to cell walls decreases
735 photosynthetic nitrogen-use efficiency. Functional Ecology 18, 419-425.

736 Onoda Y, Wright I J, Evans J R, Hikosaka K, Kitajima K, Niinemets Ü, Poorter H,
737 Tosens T, Westoby M. 2017. Physiological and structural tradeoffs underlying
738 the leaf economics spectrum. New Phytologist 214, 1447-1463.
739 Popper, Z A, Fry S, 2003. Primary cell wall composition of bryophytes and
740 charophytes. Annals of Botany 91, 1-12.
741 Preston C D, Hill MO. 1999. The geographical relationships of the British and Irish
742 flora: a comparison of pteridophytes, flowering plants, liverworts and mosses.
743 Journal of Biogeography 26, 629-642.
744 Pons T L, Westbeek M H M. 2004. Analysis of differences in photosynthetic
745 nitrogen-use efficiency between four contrasting species. Physiologia Plantarum
746 122, 68-78.
747 Poorter H, Evans J R. 1998. Photosynthetic nitrogen-use efficiency of species that
748 differ inherently in specific leaf area. Oecologia 116, 26-37.
749 Poorter H, Niinemets Ü, Poorter L, Wright I J, Villar R. 2009. Causes and
750 consequences of variation in leaf mass per area (LMA): a meta-analysis. New
751 Phytologist 182, 565-588.
752 Poorter H, Remkes C, Lambers H. 1990. Carbon and nitrogen economy of 24 wild
753 species differing in relative growth rate. Plant Physiology 94, 621-627.
754 Popper Z A, Michel G, Herve C, Domozych D S, Willats W G T, Tuohy M G,
755 Kloareg B, Stengel D B. 2011. Evolution and diversity of plant cell walls: From
756 algae to flowering plants. In: Merchant, S.S., Briggs, W.R., Ort, D. (Eds.),
757 Annual Review of Plant Biology, Vol 62, pp. 567.
758 R Core Team. 2021. R: A Language and Environment for Statistical Computing; R
759 Foundation for Statistical Computing: Vienna, Austria, Available online:
760 https://www.R-project.org/ (accessed on May 2022).
761 Reich P B, Ellsworth D S, Walters M B. 1998. Leaf structure (specific leaf area)
762 modulates photosynthesis-nitrogen relations: evidence from within and across
763 species and functional groups. Functional Ecology 12, 948-958.
764 Ren T, Weraduwage S M, Sharkey T D. 2019. Prospects for enhancing leaf
765 photosynthetic capacity by manipulating mesophyll cell morphology. Journal of
766 Experimental Botany 70, 1153-1165.
767 Ripullone F, Grassi G, Lauteri M, Borghetti M. 2003. Photosynthesis–nitrogen
768 relationships: interpretation of different patterns between Pseudotsuga menziesii

769 and Populus × euroamericana in a mini-stand experiment. Tree Physiology 23,
770 137-144.
771 Roig-Oliver M, Douthe C, Bota J, Flexas J. 2021. Cell wall thickness and composition
772 are related to photosynthesis in Antarctic mosses. Physiologia Plantarum 173,
773 1914-1925.
774 Rosseel Y. 2012. Lavaan: an R package for structural equation modeling. Journal of
775 Statistical Software 48, 1-36.
776 Shipley B, Lechowicz M J, Wright I, Reich P B. 2006. Fundamental trade-offs
777 generating the worldwide leaf economics spectrum. Ecology 87, 535-541.
778 Shipley B. 2004. Cause and correlation in biology: A user's guide to path analysis,
779 structural equations and causal inference. Cambridge University Press,
780 Cambridge, UK.
781 Smith N G, Keenan T F, Colin Prentice I, Wang H, Wright I J, Niinemets Ü, Crous K
782 Y, Domingues T F, Guerrieri R, Yoko Ishida F et al. 2019. Global photosynthetic
783 capacity is optimized to the environment. Ecology Letters 22, 506-517.
784 Takashima T, Hikosaka K, Hirose T. 2004. Photosynthesis or persistence: nitrogen
785 allocation in leaves of evergreen and deciduous Quercus species. Plant Cell and
786 Environment 27, 1047-1054.
787 Tester M, Langridge P. 2010. Breeding technologies to increase crop production in a
788 changing world. Science 327, 818-822.
789 Tosens T, Niinemets Ü, Vislap V, Eichelmann H, Castro-Díez P. 2012.
790 Developmental changes in mesophyll diffusion conductance and photosynthetic
791 capacity under different light and water availabilities in Populus tremula: how
792 structure constrains function. Plant, Cell & Environment 35, 839-856.
793 Tosens T, Nishida K, Gago J, Coopman R E, Cabrera H M, Carriquí M, Laanisto L,
794 Morales L, Nadal M, Rojas R et al. 2016. The photosynthetic capacity in 35 ferns
795 and fern allies: mesophyll CO_2 diffusion as a key trait. New Phytologist 209,
796 1576-1590.
797 von Caemmerer S, Farquhar G D. 1981. Some relationships between the biochemistry
798 of photosynthesis and the gas exchange of leaves. Planta 153, 376-387.
799 Wang M, Yuan D, Gao W, Li Y, Tan J, Zhang X. 2013. A comparative genome
800 analysis of PME and PMEI families reveals the evolution of pectin metabolism
801 in plant cell walls. Plos One 8.

802 Wang H, Prentice I C, Keenan T F, Davis T W, Wright I J, Cornwell WK, Evans B J,
803 Peng C. 2017. Towards a universal model for carbon dioxide uptake by plants.
804 Nature Plants 3, 734-741.
805 Warren C R, Adams M A. 2006. Internal conductance does not scale with
806 photosynthetic capacity: implications for carbon isotope discrimination and the
807 economics of water and nitrogen use in photosynthesis. Plant, Cell &
808 Environment 29, 192-201.
809 Warren CR, Adams M A. 2000. Trade-offs between the persistence of foliage and
810 productivity in two Pinus species. Oecologia 124, 487-494.
811 Wright I J, Reich P B, Cornelissen J H C, Falster D S, Garnier E, Hikosaka K,
812 Lamont B B, Lee W, Oleksyn J, Osada N. 2005. Assessing the generality of
813 global leaf trait relationships. New Phytologist 166, 485-496.
814 Xing K, Niinemets Ü, Rengel Z, Onoda Y, Xia J, Chen H Y H, Zhao M, Han W, Li
815 H. 2021. Global patterns of leaf construction traits and their covariation along
816 climate and soil environmental gradients. New Phytologist 232, 1648-1660.
817 Xiong D, Flexas J. 2018. Leaf economics spectrum in rice: leaf anatomical,
818 biochemical, and physiological trait trade-offs. Journal of Experimental Botany
819 69, 5599-5609.
820 Xue W, Li X, Zeng F. 2021. Inter-annual variations of seed cotton yield in relation to
821 soil organic carbon and harvest index in reclaimed desertified land. Field Crops
822 Research 272, 108267.
823 Yin L J, Xu H C, Dong S X, Chu J P, Dai X L, He M R. 2019. Optimised nitrogen
824 allocation favors improvement in canopy photosynthetic nitrogen-use efficiency:
825 Evidence from late-sown winter wheat. Environmental and Experimental Botany
826 159, 75-86.

Parsed Citations

Bahar N H A, Hayes L, Scafaro A P, Atkin O K, Evans J R. 2018. Mesophyll conductance does not contribute to greater photosynthetic rate per unit nitrogen in temperate compared with tropical evergreen wet-forest tree leaves. New Phytologist 218, 492-505.
Google Scholar: Author Only Title Only Author and Title

Bernacchi C J, Portis A R, Nakano H, von Caemmerer S, Long S P. 2002. Temperature response of mesophyll conductance. Implications for the determination of Rubisco enzyme kinetics and for limitations to photosynthesis in vivo. Plant Physiology 130, 1992-1998.
Google Scholar: Author Only Title Only Author and Title

Carriquí M, Cabrera H M, Conesa M À, Coopman R E, Douthe C, Gago J, Gallé A, Galmés J, Ribas-Carbo M, Tomás M et al. 2015. Diffusional limitations explain the lower photosynthetic capacity of ferns as compared with angiosperms in a common garden study. Plant, Cell & Environment 38, 448-460.
Google Scholar: Author Only Title Only Author and Title

Carriquí M, Roig-Oliver M, Brodribb T J, Coopman R, Gill W, Mark K, Niinemets Ü, Perera-Castro A V, Ribas-Carbó M, Sack L et al. 2019. Anatomical constraints to nonstomatal diffusion conductance and photosynthesis in lycophytes and bryophytes. New Phytologist 222, 1256-1270.
Google Scholar: Author Only Title Only Author and Title

Carriquí M, Nadal M, Clemente-Moreno MJ, Gago J, Miedes E, Flexas J. 2020. Cell wall composition strongly influences mesophyll conductance in gymnosperms. The Plant Journal 103, 1372-1385.
Google Scholar: Author Only Title Only Author and Title

Carriquí M, Nadal M, Flexas J. 2021. Acclimation of mesophyll conductance and anatomy to light during leaf aging in Arabidopsis thaliana. Physiologia Plantarum 172, 1894-1907.
Google Scholar: Author Only Title Only Author and Title

Du Q J, Liu T, Jiao X, Song X M, Zhang J Y, Li J M. 2019. Leaf anatomical adaptations have central roles in photosynthetic acclimation to humidity. Journal of Experimental Botany 70, 4949-4961.
Google Scholar: Author Only Title Only Author and Title

Ellsworth P V, Ellsworth P Z, Koteyeva N K, Cousins A B. 2018. Cell wall properties in Oryza sativa influence mesophyll CO2 conductance. New Phytologist 219, 66-76.
Google Scholar: Author Only Title Only Author and Title

Ethier G J, Livingston N J. 2004. On the need to incorporate sensitivity to CO2 transfer conductance into the Farquhar–von Caemmerer–Berry leaf photosynthesis model. Plant, Cell & Environment 27, 137-153.
Google Scholar: Author Only Title Only Author and Title

Evans J R, Kaldenhoff R, Genty B, Terashima I. 2009. Resistances along the CO2 diffusion pathway inside leaves. Journal of Experimental Botany 60, 2235-2248.
Google Scholar: Author Only Title Only Author and Title

Evans J R. 2021. Mesophyll conductance: walls, membranes and spatial complexity. New Phytologist 229, 1864-1876.
Google Scholar: Author Only Title Only Author and Title

Fan M, Shen J, Yuan L, Jiang R, Chen X, Davies W J, Zhang F. 2011. Improving crop productivity and resource use efficiency to ensure food security and environmental quality in China. Journal of Experimental Botany 63, 13-24.
Google Scholar: Author Only Title Only Author and Title

Farquhar G D, von Caemmerer S, Ball J A. 1980. A biochemical model of photosynthetic CO2 assimilation in leaves of C3 species. Planta 149, 78-90.
Google Scholar: Author Only Title Only Author and Title

Flexas J, Carriquí M. 2020. Photosynthesis and photosynthetic efficiencies along the terrestrial plant's phylogeny: lessons for improving crop photosynthesis. The Plant Journal 101, 964-978.
Google Scholar: Author Only Title Only Author and Title

Flexas J, Clemente-Moreno M J, Bota J, Brodribb T J, Gago J, Mizokami Y, Nadal M, Perera-Castro A V, Roig-Oliver M, Sugiura D et al. 2021. Cell wall thickness and composition are involved in photosynthetic limitation. Journal of Experimental Botany 72, 3971-3986.
Google Scholar: Author Only Title Only Author and Title

Gago J, Carriquí M, Nadal M, Clemente-Moreno M J, Coopman R E, Fernie A R, Flexas J. 2019. Photosynthesis optimized across land plant phylogeny. Trends in Plant Science 24, 947-958.
Google Scholar: Author Only Title Only Author and Title

Garnier E, Gobin O, Poorter H. 1995. Nitrogen productivity depends on photosynthetic nitrogen use efficiency and on nitrogen allocation within the plant. Annals of Botany 76, 667-672.
Google Scholar: Author Only Title Only Author and Title

Gómez-Ocampo G, Ploschuk E L, Mantese A, Crocco C D, Botto J F. 2021. BBX21 reduces abscisic acid sensitivity, mesophyll conductance and chloroplast electron transport capacity to increase photosynthesis and water use efficiency in potato plants cultivated under moderated drought. The Plant Journal 108, 1131-1144.
Google Scholar: Author Only Title Only Author and Title

Gvozdevaite A, Oliveras I, Domingues T F, Peprah T, Boakye M, Afriyie L, da Silva Peixoto K, de Farias J, Almeida de Oliveira E, Almeida Farias et al. 2018. Leaf-level photosynthetic capacity dynamics in relation to soil and foliar nutrients along forest–savanna boundaries in Ghana and Brazil. Tree Physiology 38, 1912-1925.
Google Scholar: Author Only Title Only Author and Title

Han J M, Lei Z Y, Flexas J, Zhang Y J, Carriqui, Zhang W F, Zhang Y L. 2018. Mesophyll conductance in cotton bracts: anatomically determined internal CO2 diffusion constraints on photosynthesis. Journal of Experimental Botany 69, 5433-5443.
Google Scholar: Author Only Title Only Author and Title

Harrison S P, Cramer W, Franklin O, Prentice I C, Wang H, Brännström Å, de Boer H, Dieckmann U, Joshi J, Keenan T F, Lavergne A. 2021. Eco-evolutionary optimality as a means to improve vegetation and land-surface models. New Phytologist 231, 2125-2141.
Google Scholar: Author Only Title Only Author and Title

Hidaka A, Kitayama K. 2009. Divergent patterns of photosynthetic phosphorus-use efficiency versus nitrogen-use efficiency of tree leaves along nutrient-availability gradients. Journal of Ecology 97, 984-991.
Google Scholar: Author Only Title Only Author and Title

Hikosaka K, Hanba Y T, Hirose T, Terashima I. 1998. Photosynthetic nitrogen-use efficiency in leaves of woody and herbaceous species. Functional Ecology 12, 896-905.
Google Scholar: Author Only Title Only Author and Title

Hikosaka K, Nagamatsu D, Ishii H S, Hirose T. 2002. Photosynthesis-nitrogen relationships in species at different altitudes on Mount Kinabalu, Malaysia. Ecological Research 17, 305-313.
Google Scholar: Author Only Title Only Author and Title

Hikosaka K. 2004. Interspecific difference in the photosynthesis-nitrogen relationship: patterns, physiological causes, and ecological importance. Journal of Plant Research 117, 481-494.
Google Scholar: Author Only Title Only Author and Title

Hikosaka K. 2010. Mechanisms underlying interspecific variation in photosynthetic capacity across wild plant species. Plant Biotechnology 27, 223-229.
Google Scholar: Author Only Title Only Author and Title

Kaldenhoff R. 2012. Mechanisms underlying CO2 diffusion in leaves. Current Opinion in Plant Biology 15, 276-281.
Google Scholar: Author Only Title Only Author and Title

Kurmangozhinov A, Xue W, Li X, Zeng F, Sabit R, Tusun T. 2020. High biomass production with abundant leaf litterfall is critical to ameliorating soil quality and productivity in reclaimed sandy desertification land. Journal of Environmental Management 263, 110373.
Google Scholar: Author Only Title Only Author and Title

Lei Z Y, Wang H, Wright I J, Zhu X-G, Niinemets Ü, Li Z-L, Sun D S, Dong N, Zhang W F, Zhou Z L et al. 2021a. Enhanced photosynthetic nitrogen use efficiency and increased nitrogen allocation to photosynthetic machinery under cotton domestication. Photosynthesis Research 150, 239-250.
Google Scholar: Author Only Title Only Author and Title

Lei Z, Liu F, Wright I J, Carriquí M, Niinemets Ü, Han J, Jia M, Atwell B J, Cai X, Zhang W et al. 2021b. Comparisons of photosynthetic and anatomical traits between wild and domesticated cotton. Journal of Experimental Botany 73, 873-885.
Google Scholar: Author Only Title Only Author and Title

Luo X, Keenan T F, Chen J M, Croft H, Colin Prentice I, Smith N G, Walker A P, Wang H, Wang R, Xu C et al. 2021. Global variation in the fraction of leaf nitrogen allocated to photosynthesis. Nature Communications 12.
Google Scholar: Author Only Title Only Author and Title

Maire V, Martre P, Kattge J, Gastal F, Esser G, Fontaine S, Soussana J F. 2012. The coordination of leaf photosynthesis links C and N fluxes in C3 plant species. Plos One 7.
Google Scholar: Author Only Title Only Author and Title

Medlyn B E, Dreyer E, Ellsworth D, Forstreuter M, Harley P C, Kirschbaum M U F, Le Roux X, Montpied P, Strassemeyer J, Walcroft A. 2002. Temperature response of parameters of a biochemically based model of photosynthesis. II. A review of experimental data. Plant, Cell & Environment 25, 1167-1179.

Google Scholar: Author Only Title Only Author and Title

Nadal M, Perera-Castro A V, Gulías J, Farrant J M, Flexas J. 2021. Resurrection plants optimize photosynthesis despite very thick cell walls by means of chloroplast distribution. Journal of Experimental Botany 72, 2600-2610.
Google Scholar: Author Only Title Only Author and Title

Niinemets Ü, Tenhunen J D. 1997. A model separating leaf structural and physiological effects on carbon gain along light gradients for the shade-tolerant species Acer saccharum. Plant, Cell & Environment 20, 845-866.
Google Scholar: Author Only Title Only Author and Title

Oguchi R, Ozaki H, Hanada K, Hikosaka K. 2016. Which plant trait explains the variations in relative growth rate and its response to elevated carbon dioxide concentration among Arabidopsis thaliana ecotypes derived from a variety of habitats? Oecologia 180, 865-876.
Google Scholar: Author Only Title Only Author and Title

Onoda Y, Hikosaka K, Hirose T. 2004. Allocation of nitrogen to cell walls decreases photosynthetic nitrogen-use efficiency. Functional Ecology 18, 419-425.
Google Scholar: Author Only Title Only Author and Title

Onoda Y, Wright I J, Evans J R, Hikosaka K, Kitajima K, Niinemets Ü, Poorter H, Tosens T, Westoby M. 2017. Physiological and structural tradeoffs underlying the leaf economics spectrum. New Phytologist 214, 1447-1463.
Google Scholar: Author Only Title Only Author and Title

Popper, Z A, Fry S, 2003. Primary cell wall composition of bryophytes and charophytes. Annals of Botany 91, 1-12.
Google Scholar: Author Only Title Only Author and Title

Preston C D, Hill MO. 1999. The geographical relationships of the British and Irish flora: a comparison of pteridophytes, flowering plants, liverworts and mosses. Journal of Biogeography 26, 629-642.
Google Scholar: Author Only Title Only Author and Title

Pons T L, Westbeek M H M. 2004. Analysis of differences in photosynthetic nitrogen-use efficiency between four contrasting species. Physiologia Plantarum 122, 68-78.
Google Scholar: Author Only Title Only Author and Title

Poorter H, Evans J R. 1998. Photosynthetic nitrogen-use efficiency of species that differ inherently in specific leaf area. Oecologia 116, 26-37.
Google Scholar: Author Only Title Only Author and Title

Poorter H, Niinemets Ü, Poorter L, Wright I J, Villar R. 2009. Causes and consequences of variation in leaf mass per area (LMA): a meta-analysis. New Phytologist 182, 565-588.
Google Scholar: Author Only Title Only Author and Title

Poorter H, Remkes C, Lambers H. 1990. Carbon and nitrogen economy of 24 wild species differing in relative growth rate. Plant Physiology 94, 621-627.
Google Scholar: Author Only Title Only Author and Title

Popper Z A, Michel G, Herve C, Domozych D S, Willats W G T, Tuohy M G, Kloareg B, Stengel D B. 2011. Evolution and diversity of plant cell walls: From algae to flowering plants. In: Merchant, S.S., Briggs, W.R., Ort, D. (Eds.), Annual Review of Plant Biology, Vol 62, pp. 567.
Google Scholar: Author Only Title Only Author and Title

R Core Team. 2021. R: A Language and Environment for Statistical Computing; R Foundation for Statistical Computing: Vienna, Austria, Available online: https://www.R-project.org/ (accessed on May 2022).

Reich P B, Ellsworth D S, Walters M B. 1998. Leaf structure (specific leaf area) modulates photosynthesis-nitrogen relations: evidence from within and across species and functional groups. Functional Ecology 12, 948-958.
Google Scholar: Author Only Title Only Author and Title

Ren T, Weraduwage S M, Sharkey T D. 2019. Prospects for enhancing leaf photosynthetic capacity by manipulating mesophyll cell morphology. Journal of Experimental Botany 70, 1153-1165.
Google Scholar: Author Only Title Only Author and Title

Ripullone F, Grassi G, Lauteri M, Borghetti M. 2003. Photosynthesis–nitrogen relationships: interpretation of different patterns between Pseudotsuga menziesii and Populus × euroamericana in a mini-stand experiment. Tree Physiology 23, 137-144.
Google Scholar: Author Only Title Only Author and Title

Roig-Oliver M, Douthe C, Bota J, Flexas J. 2021. Cell wall thickness and composition are related to photosynthesis in Antarctic mosses. Physiologia Plantarum 173, 1914-1925.
Google Scholar: Author Only Title Only Author and Title

Rosseel Y. 2012. Lavaan: an R package for structural equation modeling. Journal of Statistical Software 48, 1-36.

Google Scholar: Author Only Title Only Author and Title

Shipley B, Lechowicz M J, Wright I, Reich P B. 2006. Fundamental trade-offs generating the worldwide leaf economics spectrum. Ecology 87, 535-541.
Google Scholar: Author Only Title Only Author and Title

Shipley B. 2004. Cause and correlation in biology: A user's guide to path analysis, structural equations and causal inference. Cambridge University Press, Cambridge, UK.
Google Scholar: Author Only Title Only Author and Title

Smith N G, Keenan T F, Colin Prentice I, Wang H, Wright I J, Niinemets Ü, Crous K Y, Domingues T F, Guerrieri R, Yoko Ishida F et al. 2019. Global photosynthetic capacity is optimized to the environment. Ecology Letters 22, 506-517.
Google Scholar: Author Only Title Only Author and Title

Takashima T, Hikosaka K, Hirose T. 2004. Photosynthesis or persistence: nitrogen allocation in leaves of evergreen and deciduous Quercus species. Plant Cell and Environment 27, 1047-1054.
Google Scholar: Author Only Title Only Author and Title

Tester M, Langridge P. 2010. Breeding technologies to increase crop production in a changing world. Science 327, 818-822.
Google Scholar: Author Only Title Only Author and Title

Tosens T, Niinemets Ü, Vislap V, Eichelmann H, Castro-Díez P. 2012. Developmental changes in mesophyll diffusion conductance and photosynthetic capacity under different light and water availabilities in Populus tremula: how structure constrains function. Plant, Cell & Environment 35, 839-856.
Google Scholar: Author Only Title Only Author and Title

Tosens T, Nishida K, Gago J, Coopman R E, Cabrera H M, Carriquí M, Laanisto L, Morales L, Nadal M, Rojas R et al. 2016. The photosynthetic capacity in 35 ferns and fern allies: mesophyll CO2 diffusion as a key trait. New Phytologist 209, 1576-1590.
Google Scholar: Author Only Title Only Author and Title

von Caemmerer S, Farquhar G D. 1981. Some relationships between the biochemistry of photosynthesis and the gas exchange of leaves. Planta 153, 376-387.
Google Scholar: Author Only Title Only Author and Title

Wang M, Yuan D, Gao W, Li Y, Tan J, Zhang X. 2013. A comparative genome analysis of PME and PMEI families reveals the evolution of pectin metabolism in plant cell walls. Plos One 8.
Google Scholar: Author Only Title Only Author and Title

Wang H, Prentice I C, Keenan T F, Davis T W, Wright I J, Cornwell WK, Evans B J, Peng C. 2017. Towards a universal model for carbon dioxide uptake by plants. Nature Plants 3, 734-741.
Google Scholar: Author Only Title Only Author and Title

Warren C R, Adams M A. 2006. Internal conductance does not scale with photosynthetic capacity: implications for carbon isotope discrimination and the economics of water and nitrogen use in photosynthesis. Plant, Cell & Environment 29, 192-201.
Google Scholar: Author Only Title Only Author and Title

Warren CR, Adams M A. 2000. Trade-offs between the persistence of foliage and productivity in two Pinus species. Oecologia 124, 487-494.
Google Scholar: Author Only Title Only Author and Title

Wright I J, Reich P B, Cornelissen J H C, Falster D S, Garnier E, Hikosaka K, Lamont B B, Lee W, Oleksyn J, Osada N. 2005. Assessing the generality of global leaf trait relationships. New Phytologist 166, 485-496.
Google Scholar: Author Only Title Only Author and Title

Xing K, Niinemets Ü, Rengel Z, Onoda Y, Xia J, Chen H Y H, Zhao M, Han W, Li H. 2021. Global patterns of leaf construction traits and their covariation along climate and soil environmental gradients. New Phytologist 232, 1648-1660.
Google Scholar: Author Only Title Only Author and Title

Xiong D, Flexas J. 2018. Leaf economics spectrum in rice: leaf anatomical, biochemical, and physiological trait trade-offs. Journal of Experimental Botany 69, 5599-5609.
Google Scholar: Author Only Title Only Author and Title

Xue W, Li X, Zeng F. 2021. Inter-annual variations of seed cotton yield in relation to soil organic carbon and harvest index in reclaimed desertified land. Field Crops Research 272, 108267.
Google Scholar: Author Only Title Only Author and Title

Yin L J, Xu H C, Dong S X, Chu J P, Dai X L, He M R. 2019. Optimised nitrogen allocation favors improvement in canopy photosynthetic nitrogen-use efficiency: Evidence from late-sown winter wheat. Environmental and Experimental Botany 159, 75-86.
Google Scholar: Author Only Title Only Author and Title